Revista Brasileira de Física, Vol. 8, Nº 3, 1978

Some Considerations Upon the Emission Line Spectrum of the Crab Nebula

S. M. V. ALDROVANDI*
Instituto Astronômico e Geofísico, USP, São Paulo

and

G. STASINSKA**
Département d'Astrophysique Fondamentale, Observatoire de Meudon, Meudon, France

Recebido em 22 de Dezembro de 1977

We present a detailed program of transfer of ionizing radiation in a diluted medium, in which the equations of thermal balance and ionization equilibriurn are solved. This program allows to build models of various types of objects, like nuclei of galaxies, supernova remnants, H II regions or planetary nebulae, and to calculate their emission line spectra. When applying this program to the Crab Nebula, a supernova remnant with a well observed filamentary structure, we were lead to the following conclusions: a detailed model of this should try to depict individual filaments (which have different densities and lie at different distances from the ionizing source), and not only a "mean" filament. lrhe He II λ 4686 line which was predicted much weaker than observed in all previous models seems to come not only from the filaments but also from the diluted medium in which the filaments are bathing.

Apresentamos neste trabalho um programa detalhado de transporte da radiação ionizante em um meio diluído para o qual as equações de ioniza-

* Postal acldress: Instituto Astronômico e Geofísico U.S.P., Caixa Postal 30627, BR-01000 São Paulo (SP), Brazil.

**Département d'Astrophysique Fondamentale, Observatoire de Meudon F-92190 Meudon, France.

ção e de balanceamento térmico são resolvidas. Esse programa permite a construção de modelos para vários tipos de objetos tais como núcleos de galáxias, restos de supernovas, regiões H II e nebulosas planetárias, calculando o espectro de linhas em emissão. Aplicando tal programa à Nebulosa de Caranguejo, um resto de supernova com estrutura filamentar bem conhecida, chegamos às seguintes conclusões: um modelo detalhado do objeto deve tentar descrever cada filamento individualmente e não um filamento "médio", pois cada um tem uma densidade diferente e se localiza a uma distancia diferente da fonte ionizante; a linha do He II λ4686, cuja intensidade calculada em modelos precedentes era muito menor que a intensidade observada, parece ser emitida em parte por um meio difuído no qual estariam mergulhados os filamentos.

1. INTRODUCTION

The Crab Nebula is a supernova remnant presenting a well observed filamentary structure and a strong continuum of non-thermai radiation extending from the radio region up to the X-rays. Its emission line spectrum has been the subject of several theoretical studies[1,2,3,4]. Its chemical composition has been only roughly determined, because, as has been shown by Davidson[3], the intensities of the observed lines depend only slightly on the elemental abundances. A detailed model should try to depict individual filaments, and *not* only an "average" filament, since the line intensity ratios vary by large factors from one filament to another (see Woltjer[5] and Trimble[6]). An effort in this direction has been done recently by Contini, Kozlovsky and Shaviv[4]. In all the models constructed so far, the large intensity observed for the He II recombination line at h 4686 Å remained unexplained.

In this paper we wish to draw attention on several points which should be taken into account, while constructing more detailed models of the Crab Nebula, when further observations become available.

In Section 2 we describe the numerical program treating the transfer of the radiation and give the references to the atomic data which have been used. In Section 3, we summarize the relevant observational re-

sults. In Section 4, we build a simple model for the "mean" filamentas described by Woltjer[5], and briefly discuss the relative importance of several assumptions in the numerical treatment of this particular problem. We also examine the importance of varying the gas density and the distance to the ionization source when building models of individual filaments. In section 5 we show the possible influence on the nebular emission spectrum of a diluted gas which could bepresent between the filanients. Finally, we present our concluding remarks in Section 6.

2. THE NIJMERICAL PROGRAM AND ATOMIC DATA

The program calculates the ionization and temperature structure of a gas submitted to a flux of ionizing photons and provides the intensities of the emission lines. It can be applied to a large variety of objects (quasars or nuclei of galaxies as well as galactic objects), and has already been used in a study of the planetary nebula NGC 7027[7] and in studies on H II regions[8,9]. The method of computation is similar to that of Tarter[10] or Mac Alpine[11].

A model is obtained after choosing the following input parameters: the spectrum and power of the source of ionization, the density distributions of the gas and its chemical composition. The elements considered sofar are H, He, C, N, O, Ne, Mg and S. It is possible to include purely absorbing dust provided that one assumes its absorption properties. The calculations begin at the inner boundary of the gas or at a distance R_0 from the source where the optical depth to ionizing radiation is small and the emission by the volume situated between the source and R_0 negligible. The physical conditions at R_0 are obtained by solving the coupled equations of ionization and thermal balance. Then the radiation field is calculated and the physical conditions are determined at a distance $R_0 + \Delta R$. This process is repeated until a given requirement is fulfilled (e.g. the outer boundary of the object has been reached or hydrogen has become essentially neutra1 and the temperature has dropped below 100 K).

In the following, we give a complete description of the numerical pro-

gram. In practice, depending on the problem treated, several processes, if negligible, can be omitted in the calculations.

a) The Radiation Field

Let $J_E(\vec{R})$ be the total mean intensity between energies E and E + dE at point $\vec{R}$ in the nebula. We have:

$$J_E(\vec{R}) = J_E^S(\vec{R}) + J_E^D(\vec{R}) \tag{1}$$

where $J_E^S(\vec{R})$ is the mean intensity due to the source of ionization, and $J_E^D(\vec{R})$ is that due to the diffuse radiation.

1) Spherical Symmetry

If spherical symmetry is assumed around a central source, then the primary radiation is given by:

$$4\pi\, J_E^S(\vec{R}) = f(\tau_E^a,\ \tau^S)\ L_E/4\pi\, R^2 \tag{2}$$

L_E being the number of photons emitted by the primary source between E and $E + dE$, per unit time, and $f(\tau_E^a,\ \tau^S)$ a function of the absorption optical depth τ^S. and of the optical depth due to electron scattering τ^S, given by Tarter and Salpeter[12]. The optical depths are calculated by the following expressions:

$$\tau_E^a = \int_{R_0}^{R} \Big(\sum_{ij} n_{ij}(r)\ \sigma_{ij}(E) \Big) dr \tag{3}$$

and

$$\tau^S = \int_{R_0}^{R} n_e(r)\ \sigma^S\, dr \tag{4}$$

where $n_{ij}(r)$ is the numerical density of ion j of element i at the distance r from the source, $\sigma_{ij}(E)$ is the total photoionization cross-section of the ion (i,j), i.e. the sum of the cross sections for valence

and internal shells; $n_e(r)$ is the electronic density, σ^S the Thomson cross section.

The cross sections concerning valence shells were taken from references summerized by Osterbrock[13] for H, He, C, N, O, Ne and by Aldrovandi and Péquignot[14] for Mg and S. The K-shell ionization cross sections of the heavy elements were calculated according to Bergeron and Collin-Souffrin[15]. Owing to the lack of good data, ionization of the 2s subshells in heavy elements has been ignored. This was considered permissible, considering the uncertainties in the adopted cross sections at high frequencies. A revision of photoionization cross sections is in progress, taking into account recently obtained results.

Theoretically, the diffuse radiation is given by:

$$4\pi J_E^D(\vec{R}) = \int_V j_E(\vec{r}) \exp(-\tau_E^a(\vec{R},\vec{r}))\, d\vec{r} , \qquad (5)$$

where V is the volume of the whole nebula, $j_E(\vec{r})$ is the gas emissivity at point r between energies E and E + dE and $\tau_E^a(\vec{R},\vec{r})$ is the optical depth corresponding to the segment $|\vec{R}-\vec{r}|$ (scattering of the secondary photons is neglected for the sake of simplicity; it happens that this is a reasonable assumption[10]). To minimize computing time and storage, the transfer of the diffuse ionizing radiation is solved using the "outward only" approximation of Tarter[10], in which the emission at any point is distributed isotropically in the outward directions. This approximation is partly justified by the optical conditions in the gas; if the gas is optically thin at a given frequency out to a certain distance R of the source, then an inward moving photon of this frequency, emitted at a distance R, would not be reabsorbed until reaching this distance R on the other side of the nebula. In the other extreme, if the gas is optically thick near $\vec{R}$, then an inward moving photon would be reabsorbed very close to the point where it has been emitted. In the "outward only" approximation', the volume of integration in Equation (5) is then replaced by a sphere of diameter equal to R, passing by the centre of the nebula (see Fig. 1) and the point $\vec{R}$. Thomson scattering of the secondary photons is neglected.

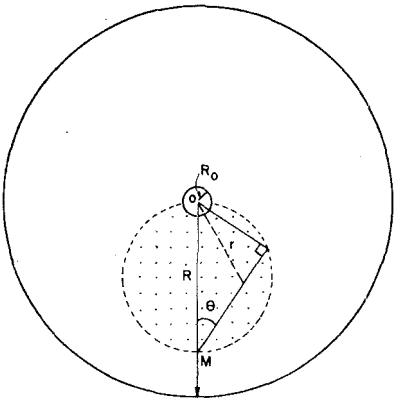

Fig.1 - Model with spherical symmetry. The dotted circle represents the volume V over which is performed the integration to calculate the diffuse radiation field at point *M* (see Eq. 5).

2) Plane Parallel Symmetry

If the thickness of the ionized gas layer is much smaller than the distance to the ionizing source, or if the source is located outside the gas cloud, then plane paralell symmetry may be better suited for treating the problem. Our program is adaptable to this case, with the primary radiation normally incident on the gas layer. The same considerations as above lead to treat the ionizing diffuse radiation field inthe following manner: in the case of a gas cloud illuminated from outside, the ionizing photons emitted towards the source are neglected, since they are supposed to be lost for the cloud; in the case of a sheet of gas surrounding the source, the emission is supposed to be concentrated isotropically outwards, like in the spherical case. In any practical case, a more sophisticated treatment can be used when the geometry and the physical conditions require it.

The diffuse - or secondary - ionizing radiation field includes continuous and line radiation produced by free-free transitions, recombinations to the ground state of all ions, recombinations to excited states and subsequent cascades which produce photons with energies greater than 13.6 eV, and by the 1s - 2s two-photon emission of helium ions.

The free-free emissivity is taken from Seaton[16]. The emissivity due to recombination is:

$$J_E(\vec{r}) = n_e(\vec{r}) \sum_{ij} n_{ij}(\vec{r}) (\alpha_{n_v}(E) + \sum_{n>n_v} \alpha_n \ (E > 13.6 \text{ eV})) \qquad (6)$$

where n_v is the principal quantum number of the ground state of ion (i,j), and

$$\alpha_n(E) = 8.2 \times 10^7 \frac{g_j}{g_{j+1}} E^2 \ T^{-3/2} \ \sigma_{ij}^n(E) \ \exp((I_n - E)/kT) \qquad (7)$$

in units of $cm^3 \ s^{-1} \ eV^{-1}$, g_j being the statistical weight of ion (i,j), $\sigma_{ij}^n(E)$ the photoionization cross-section of the n-shell, I_n the ionization potential of the n-shell and T_e the electronic temperature. For $n = n_v$, the $\sigma_{ij}^n(E)$ are the photoionization cross-section of the valence shells meritioned before; for $n > n_v$, the hydrogenic approximation is taken[17]. The ionizing line radiation field was calculated in the simplified following manner: we considered for each ion the permitted transitions arising from the lowest excited state whith change of the principal quantum number n, and eventually those arising from the lowest excited state with the same n. The first were assumed to be produced by recombinations to the excited levels (directly orafter cascade), and by collisional excitations, the second only by collisional excitations. For He II, it was assumed that a certain fraction ($-\frac{1}{3}$ of the recombinations lead to populate the 2^2S level, producing two-quantum emission[18]. Collisionally induced transitions $2^2S \rightarrow 2^2P$ were neglected, which is a good approximation as long as n_e is less than $4 \times 10^5 \ cm^{-3}$.

Concerning He I, it was assumed that all recombinations lead to populate the 2^1P level or the 2^3S level, producing a photon of $\simeq 20$ eV. The tyo-photon emission was neglected sofar, but it becomes important relatively to one photon emission at densities larger than $5 \times 10^3 \ cm^{-3}$ when collisions induce the $2^3S \rightarrow 2^1S$ transition. Resonance scattering was neglected, as it was assumed that the resonance photons scatter immedia-

tely out of the line, so that their path length is determined only by absorption. This point however is open to discussion.

A more detailed treatment of the diffuse radiation field of He I and He II is under study, which in particular will take into accbunt the destruction of the $2^1P \rightarrow 1^1S$ photons of He I by radiative $2^1P \rightarrow 2^1S$ decay, the $2^1S \rightarrow 1^1S$ two photon emission of He I, and the destruction of the $2^2P^0 \rightarrow 1^2S$ photons of He II by the Bowen resonance fluorescence mechanism[13].

b) Ionization and Thermal Balance

The mechanisms considered in the ionization equilibrium are the following:

i) photoionization due to primary and secondary radiation, removing a valence electron;

ii) photoionization removing an electron from an internal shell (for ions with more than two electrons) followed by the removal of a second electron by Auger effect for ions with more than three electrons[19];

iii) collisional ionization by thermal electrons;

iv) radiative and dielectronic recombination;

v) charge exchange reactions between hydrogen and heavy elements, when the corresponding data are available;

vi) collisional ionization of hydrogen and heliuni by the electrons provided by photoionizations.

References for the photoionization cross-sectionç which were used have been given above. The collisional ionization coefficients were taken from Tucker and Gould[20] with the screen factor correction proposed by House[21].

The mean number of collisional ionizations by the photoelectrons was taken from Bergeron and Collin-Souffrin[22]. The recombination coefficients were taken from Aldrovandi and Péquignot[14,23].

The heatirig of the gas is due to the interaction between the thermal electrons and electrons supplied by photoionization due to primary and diffuse radiation, and by the Auger effect.

The cooling mechanisms considered are the following:

i) collisional excitation of ions by thermal electrons and by hydrogen atoms, with a subsequent emission of an allowed, semi-forbidden or forbidden line. In the two latter cases, the equations of statistical equilibrium were solved for the energy levels (up to five) concerned by the transition. In the case of permitted lines, each collision was assumed to be directly followed by a photon emission.

ii) radiative and dielectronic recombination.

iii) collisional ionization by thermal electrons.

iv) free-free transitions by thermal electrons.

The atomic data concerning free-free radiation, and thermal ionization and excitation of permitted lines were taken from works mentioned by Aldrovandi and Péquignot[24]. The Lyman a excitation rate of hydrogen was calculated according to Johnson[25]. Transition probabilities of forbidden lines were taken from Wiese et *al.*[26,27], except those concerning the C I isoelectronic sequence which were taken from Nussbaumer[28]. Those of the semi-forbidden lines of the CIII isoelectronic sequence were taken from Garstang and Shamey[29]. The references for the collision strengths of forbidden and semi-forbidden lines are given in more convenient form in Table 1.

Table I

ion	transition	reference
C I	$2p^2 - 2p^2$ ($^1D - {}^1S$; $^3P - {}^1S$; $^3P - {}^1D$)	a
C I	$2p^2 - 2p^2$ ($^3P_2 - {}^3P_1$; $^3P_2 - {}^3P_0$; $^3P_1 - {}^3P_0$)	b
C II	$2s^22p - 2s2p^2$ ($^2P - {}^4P$)	c
C II	$2p - 2p$ ($^2P_{1/2}$, $^2P_{3/2}$)	d + b
C III	$2s^2 - 2s2p$ ($^1S - {}^3P$)	e
N I	$2p^3 - 2p^3$ ($^2D - {}^2P$; $^2S - {}^4P$; $^4S - {}^2D$)	a
N II	$2p^2 - 2p^2$ ($^1D - {}^1S$; $^3P - {}^1S$; $^3P - {}^1D$)	f
N II	$2p^2 - 2p^2$ ($^3P_1 - {}^3P_2$; $^3P_0 - {}^3P_2$; $^3P_0 - {}^3P_1$)	d
N III	$2s^22p - 2s2p^2$ ($^2P - {}^4P$)	c
N III	$2p - 2p$ ($^2P_{1/2} - {}^2P_{3/2}$)	d
N IV	$2s^2 - 2s2p$ ($^1S - {}^3P$)	g
O I	$2p^4 - 2p^4$ ($^1D - {}^1S$; $^3P - {}^1S$; $^3P - {}^1D$)	a
O I	$2p^4 - 2p^4$ ($^3P_1 - {}^3P_0$; $^3P_2 - {}^3P_0$; $^3P_2 - {}^3P_1$)	h + b
O II	$2p^3 - 2p^3$ ($^2D - {}^2P$; $^4S - {}^2P$; $^4S - {}^2D$)	i
O III	$2p^2 - 2p^2$ ($^1D - {}^1S$; $^3P - {}^1S$; $^3P - {}^1D$)	j
O III	$2p^2 - 2p^2$ ($^3P_1 - {}^3P_2$; $^3P_0 - {}^3P_2$; $^3P_0 - {}^3P_1$)	d
O IV	$2s^22p - 2s2p^2$ ($^2P - {}^4P$)	c
O IV	$2p - 2p$ ($^2P_{1/2} - {}^2P_{3/2}$)	d
O V	$2s^2 - 2s2p$ ($^1S - {}^3P$)	g
Ne II	$2p - 2p$ ($^2P_{3/2} - {}^2P_{1/2}$)	d
Ne III	$2p^4 - 2p^4$ ($^1D - {}^1S$; $^3P - {}^1S$; $^3P - {}^1D$)	k
Ne III	$2p^4 - 2p^4$ ($^3P_1 - {}^3P_0$; $^3P_2 - {}^3P_0$; $^3P_2 - {}^3P_1$)	d
Ne IV	$2p^3 - 2p^3$ ($^2D - {}^2P$; $^4S - {}^2P$; $^4S - {}^2D$)	d

Table I (suite)

ion	transition	reference
Ne V	$2p^2 - 2p^2$ ($^1D - {}^1S$; $^3P - {}^1S$; $^3P - {}^1D$)	d
Ne V	$2p^2 - 2p^2$ ($^3P_1 - {}^3P_2$; $^3P_0 - {}^3P_2$; $^3P_0 - {}^3P_1$)	d
Ne VI	$2s^22p - 2s2p^2$ ($^2P - {}^4P$)	c
Ne VI	$2p - 2p$ ($^2P_{1/2} - {}^2P_{3/2}$)	d
Ne VII	$2s^2 - 2s^2p$ ($^1S - {}^3P$)	g
Mg IV	$2p^5 - 2p^5$ ($^2P_{3/2} - {}^2P_{1/2}$)	d
Mg V	$2p^4 - 2p^4$ ($^1D - {}^1S$; $^3P - {}^1S$; $^3P - {}^1D$)	d
Mg V	$2p^4 - 2p^4$ ($^3P_1 - {}^3P_0$; $^3P_2 - {}^3P_0$; $^3P_2 - {}^3P_1$)	d
Mg VI	$2p^2 - 2p^3$ ($^2D - {}^2P$; $^4S - {}^2P$; $^4S - {}^2D$)	d
Mg VII	$2p^2 - 2p^2$($^3P_1 - {}^3P_2$; $^3P_0 - {}^3P_2$; $^3P_0 - {}^3P_1$)	extrapolated from d
S II	$3p^3 - 3p^3$ ($^2D - {}^2P$; $^4S - {}^2P$; $^4S - {}^2D$)	i
S III	$3p^2 - 3p^2$ ($^1D - {}^1S$; $^3P - {}^1S$; $^3P - {}^1D$)	i
S III	$3p^2 - 3p^2$ ($^3P_1 - {}^3P_0$; $^3P_2 - {}^3P_0$; $^3P_2 - {}^3P_1$)	i
S IV	$3p - 3p$ ($^2P_{3/2} - {}^2P_{1/2}$)	m

a Aldrovandi, S.M.V., Péquignot, D., Astron.Astrophys. 50,141 (1976), after cross-sections calculated by Le Dourneuf, M. 1976, thesis.

b Penston, M.V., Astrophys.J. 162, 771 (1970). (collisions with HI).

c Osterbrock, D.E. in *Nuclei of Galaxies* (Vatican) p. 151 (1971).

d Saraph, H.E., Seaton, M.J., Shemming, J., Phil.Trans.Roy.Soc. Lon. A 264, 77 (1969).

e Flower, D.R., Launay, J.M., Astron. Astrophys. 29, 321 (1973).

f Seaton, M.J., M.N.R.A.S. 170, 475 (1975).

g Osterbrock, D.E., Journ. Phys. B., 3, 149 (1970).

h Le Dcurneuf, M., Nesbet, R.K., Journ. Phys. B, 9, L241 (1976).

i Pradhan, A.K., M.N.R.A.S. 177, 31 (1976).

j Eissner, W., Seaton, M.J., Journ. Phys. B, 7, 2533 (1974).

k Pradhan, A.K., Journ. Phys. B 7, L503 (1974).
l Krueger, T. K., Csyzak, S. J., Proc. Roy. Soc. Lon. A 318, 531 (1970).
m Brocklehurst, M. M.N.R.A.S. 160, 19 P. (1972).

c) The Observable Emission Line Spectrum

The emissivities of the visible recombination lines of H I, He I and He II were calculated at each step according to Brocklehurst[30,31]. For the heavy elements, we calculated only the emissivities of the lines produced by collisional excitation. For these lines, the contribution of recombinations is negligible. The observable line spectrum emitted bythe nebula is obtained by integrating the emissivities over the whole volume of the gas cloud or by integrating the emissivities along the lineof sight at different projected distances from the centre. All possible reabsorption effects were neglected, except in the case of H I and He II for which Baker and Menzel's case *B* is taken.

d) Numerical Methods

In order' to calculate the ionizing and heating rates, the integralsover energy were performed with the trapezoidal rule using 126 points carefully distributed between 10 eV and 1360 eV, and up to 40 points when necessary in.the higher energy range. At the point:; of discontinuity in the prirnary or in the diffuse radiation, the function to integrate was evaluated on both sides of the discontinuity. The contribution of the lines was treated separately.

Concerning the opacity, the optical depths τ_E^a and τ^S defined by Equations (3) and (4) have to be calculated with as much accuracy as possible. Indeed, an underestimate of the optical depth at a given point would produce an overestimate in the ionizing flux at this point, whence an overestimate of the ionization degree of the gas, so that the érror is self-propagating. We calculated the quantities .

$$y_{ij} = \int_{R_0}^{R} n_{ij}(r)\, dr \qquad \text{and} \qquad y_e = \int_{R_0}^{R} n_e(r)\, dr$$

appearing in Equations (3) and (4), where n_{ij} and n_e are functionals of all the y_{ij} and y_e, with a computer program constructed Krogh[32] using a predictor-corrector method with variable integration step. The total number of steps for one model is generally comprised between 60 and 100.

To compute the diffuse radiation, the angular interval ($0 \leq \theta \leq \frac{\pi}{2}$, see Fig. 1) was divided into five bands and the angular integration was performed using the trapezoidal rule.

The ionic abundances and electronic temperature were obtained by solving the ooupled equations of ionization and thermal equilibrium using appropriate iterative methods.

e) Accuracy

It is extremely difficult to account for the accuracy of such models. Severa1 kinds of errors have to be distinguished: those due to the neglect of some important physical process, those arising from inaccuracies in the atomic data, and those coming from the numerical methods. Among the latest, the errors on the integrals over energy and those on the temperature and ionic populations at a given point are probably less than a few percent; the errors on the diffuse radiation field or on the optical depth are much more difficult to estimate. However, we believe that the errors due to inaccuracies in the atomic data and to the omission of some physical processes are dominant in most cases.

3. OBSERVATIONAL DATA

The Crab Nebula appears like an ellipse with axes of about 4' and 6 mi-

nutes of arc. It lies at a distance of about 2 kpc, and the filaments are distributed throughout its volume (as demonstrated by Trimble[33]).

The nebula emits a strong continuum radiation which has been observed from the radio frequency range up to the X-ray domain. The continuum spectrum may be represented by a power-law with increasing spectral index towards higher frequencies[34]. Since the extrapolation of the X-rays intersects the optical continuum just beyond the observed wavelength range, it is reasonable to assume that the ultraviolet continuum isthe extrapolated X-ray continuum[34]. To compute the ionization structure of the nebula, we therefore adopt for the UV and X-ray flux density at the Earth:

$$I(E) = 9.8\ E^{-2.1} \text{ photons/cm}^2\text{/s/keV} \qquad (8)$$

where E is the photon energy in keV.

The Hβ flux of the entire nebula is $7.5\ 10^{-11}$ ergs/cm^2/s (Ref.34), assuming a visual extinction A_V = 1.6 mag/kpc (as determined by Miller[35]).

The filaments of the Crab Nebula have been observed by Woltjer[5] and Trimble[6]. In spite of the differences in the emission spectra from one filament to another, a first approach can justify a model based on the spectrum of an average filament, as defined by Woltjer[5]. In the first line of Table 2, we give the line intensities of a mean filament, relatively to Hβ, following Woltjer's data, except for [O I] which is taken from Trimble[33]. Woltjer's line intensities were obtained assuming that the continuum varies as $\nu^{-1.15}$. However, recent measurements of the continuum[34,35] corrected from reddening[35] reveal a much less steep visible continuum. Therefore, we give in the second line of Table 2 the line intensities which are obtained when considering a variation of the continuum represented by $\nu^{-0.41}$, according to Kirshner[34]. It should also be noted that actually, the [N II] λλ 6584, 6548 line was not observed by Woltjer, but only estimated from a comparison between Ha and the weaker [N II] line by Minkowsky[36], Ha being deduced from Hβ using a theoretical Balmer decrement. Trimble[6] suggests that the [N II] intensity should be decreased somewhat; the figure appearing for [N II] in the se-

cond line of Table 2 would then be ~ 8. These corrections, however, are not of mucti consequence when dealing with an "average" filament.

As for the He II λ 4686 line, it seems in fact to be blended with a [Fe III] line at λ 4658 Å (Ref.6), but it is difficult to estimate the contribution of the [Fe III] line.

The electronic density in the filaments has been determined by Osterbrock[37], from the [O II] λ 3729 / [O II] λ 3726 line ratio. Its value ranges froni v 500 cm^{-3} up to 3700 cm^{-3}.

4. MODELS OF FILAMENTS

a) Model 1: The Average Filament

Since the mean distance of the filament to the nebular centre is much larger than their thickness, we adopt the plane-parallel approximation; we assume that the ionizing radiation described by Equation (8) reaches normally the plane boundary of the filament located at a distance of 4×10^{18} cm from the source. The ionizing diffuse radiationreemitted backwards is ignored. This approximation is shown to be justified by Contini et al.[4]. Charge exchange reactions have been considered only between O^+ and H^0 (Ref.38). The hydrogen density is taken constant and equal to 10^3 cm^{-3}. As we do not pretend to build a proper model of the nebula, we considered only 6 elements: H, He, C, N, O, Ne.

With the following relative abundances: 1; 0.45; 3×10^{-4}; 1×10^{-4}; 7×10^{-4}; 2×10^{-4}, we found that except for He II λ 4686 which was found weaker than observed by a factor about 5, we could satisfactorily reproduce the observed spectrum considering the observational errors and the not very meaningful definition of an average filament. The problem of the He II line is postposed to the next section.

The third line of Table 2 gives the line intensities relatively to Hβ at a depth in the filament of $z = 1 \times 10^{16}$ cm. The fourth line corres-

Table 2 - Line intensities relatively to Hβ

	C IV λ 1549	C III λ 1909	C II λ 2325	O II λ 3727	Ne III λ3869 + λ3967	O III λ 4363	He I λ 4471	He II λ 4686	O III λ5007 + λ4959	N I λ 5200	O I λ6300 + λ6364	N II λ6548 + λ6584
Obs. Woltjer				9.7	1.5		.18	.73	14.7		1.4	13.3
Obs. Woltjer corrected				11.8	1.8		.19	.75	14.4		1.4	10.7
Model 1 (at $z = 10^{16}$ cm)	4.9(-2)	.78	9.1	14.7	1.9	.10	.23	.17	15.9	.15	1.7	7.6
Model 2 (at $z = 2 \times 10^{16}$ cm)	7.5(-2)	.82	11.2	14.8	2.2	.10	.23	.17	15.9	.40	3.1	8.4
Model 2	1.2(-3)	7.5(-2)	6.6	9.9	.40	7.8(-3)	.22	.03	1.9	.48	5.7	10.2
Model 3	.94	3.7	6.8	9.0	3.2	.32	.22	.28	34.9	.10	1.1	4.1
Diluted medium	56.4	26.2	1.4	9.0(-2)	.32	.27	3.1(-2)	4.4	9.7	1.7(-5)	3.0(-6)	4.5(-2)
Model 1 + diluted medium (see text)	9.35	5.0	9.8	12.7	1.9	.13	.20	.87	16.1	.34	2.6	7.2
Obs. Miller				12.6	1.9	.19	.28	.68	15.8		1.5	5.5

ponds to a depth of $z = 2 \times 10^{16}$ cm. The calculated intensities of several lines of interest which have not yet been observed are reportedas well. Figures 2 and 3 display the temperature distribution and the fractional abundances of the ions respectively, versus the distance z tothe illuminated boundary.

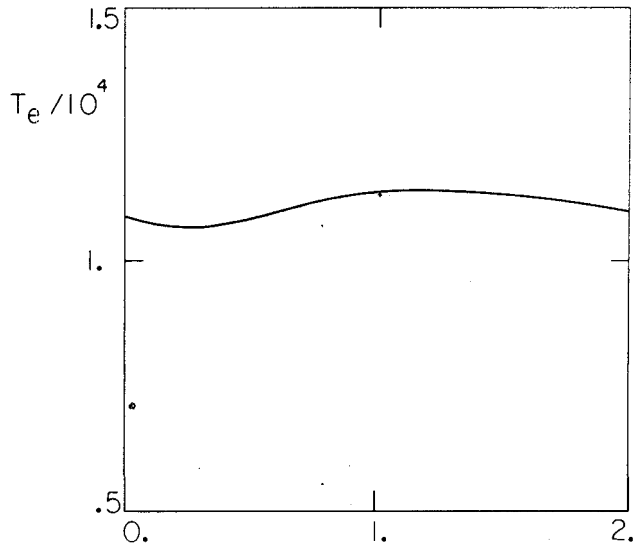

Fig. 2 - Electronic temperature versus distance z to the illuminated boundary in the model of the "mean" filament.

From these figures, we see tnat there is a large zone where hydrogen is weakly ionized but the temperature still high (~ 10^4 K). The heavy elements remain ionized at larger z than hydrogen, except oxygen which becomes neutral together with hydrogen owing to charge exchange between O^+ and H^0, aiid carbon which ionization potential is less than 13.6 eV. Therefore, certain lines of heavy elements like [N II], [Ne III] and especially [O I] and [N I] .are still produced while Hβ is no more emitted, and their intensities relatively to Hβ vary with z as seen by comparing lines 3 aiid 4 in Table 2. But the ratio [O II]/[O III] remainsconstant as soonas the [O I] line appears, reflecting that neutral hydrogen is present. The intensity of the observed [O I] line gives an information about the quantity of neutral matter, and therefrom on the proportionof the [N II] line emitted in the neutra1 region.

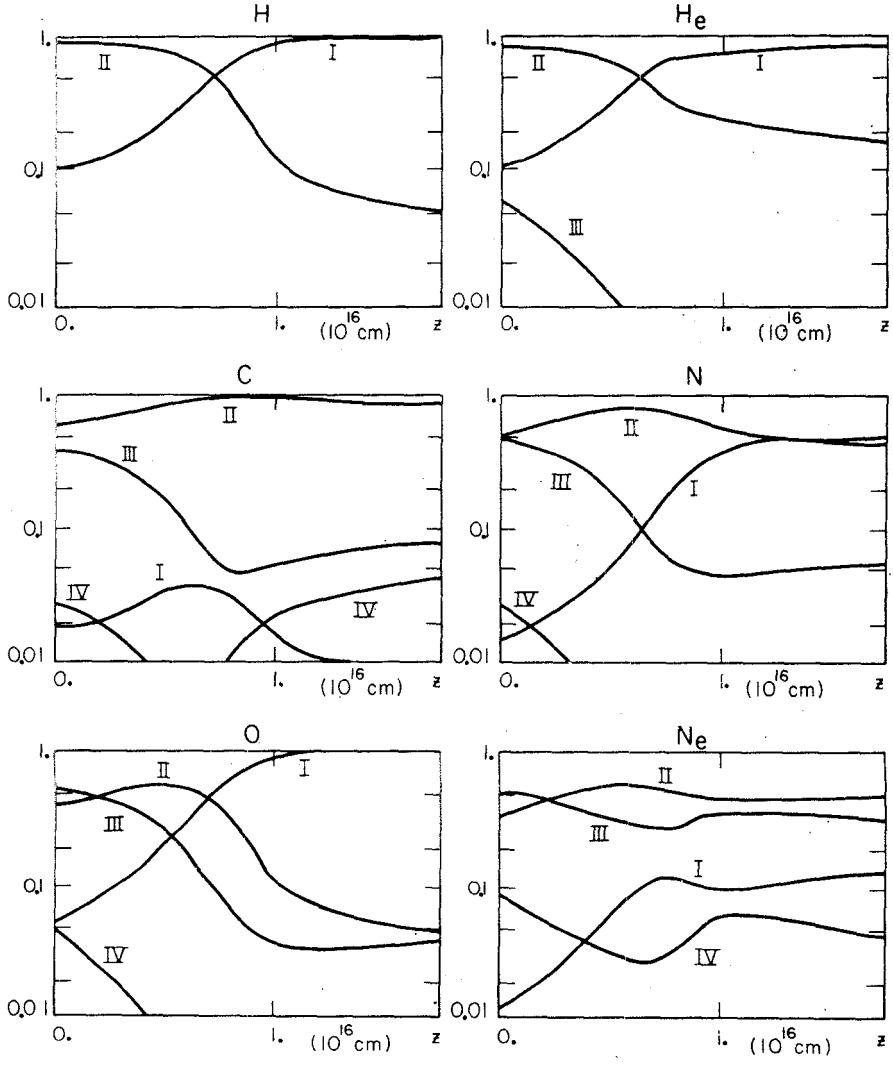

Fig. 3 - Fractional abundance of the ions versus z in the model of the "mean" filament.

It is worthwhile noting that in this model, the absorption by heavy elements ($Z \geq 6$) is completely negligible, as well as the energy gains due to their photoionization. But the heavy elements produce a diffuse radiation which slightly influences the ionization structure (a model where this was ignored gave line intensities different by about 20% from those of the model presented in Table 2).

The ionization of K-shells becomes important for positive ions of carbon and nitrogen when most of low frequency radiation has been absorbed. The ionization of *K*-shells may then be more efficient than the ionization of valence shells by factors as large as ~ 6. A simple consideration of the ionization equilibrium equations demonstrates that modification of the ionization rate of a given ion changes the abundances of the trace ions involved in the equilibrium, but keeps the abundance of the other ions constant. Since ionizations of K-shells are followed by Auger effect which generally removes one additional electron, K-shell ionization strongly influence the abundances of the C II, C V, NIV, N V and N VI ions. Among these, none is likely to be observed, except maybe C IV. A model where ionization of K-shells was ignored gave C IV λ 1549 / H$\beta \simeq 2.7 \times 10^{-2}$, 3 times lower than in the initial model, the intensities of the other lines remaining unchanged, because C IV contributes very little to the cooling. Therefore, neglect of *K*-shell ionizations in the filamerits of the Crab Nebula (as has been done by Contini *et al.*[4] for example), is quite permissible if one is not interested in the C IV λ 1549 line.

We verifiecl that for the filaments of the Crab Nebula, secondary electrons have no influence on the ionization structure and line spectrum. Indeed, ionization due to secondary electrons becomes efficient with respect to photoionization by the primary radiation (multiplying the ionization rates due to primary radiation by ~ 4 for H^0 and 1.5 for He^0) only in the region where H and He are already completely neutral. Besides, the ionization of H^0 is dominated by the photons due to the recombination of He^+, owing to their large abundance.

b) The Influence of Density and Position Upon the Spectrum Emitted by a Filament.

The fact that the gas density in a filament and the luminosity of the source of ionization would influence the spectrum emitted by the filament has already been shown by Davidson[3]. This author defined a parameter U_1 (incident energy flux per photon energy interval at 13.6 eV, divided by the electronic density), though allowed it to vary only between 1.5×10^6 cm/s and 8.5×10^6 cm/s. But Osterbrock's[37] estimates of the electronic density varied by factors up to 7 from one filament to another. Besides, the filaments observed by Woltjer[5] or Trimble[6] are located at various distances to the source. Contini *et al.*[4] tried to account for the spectra of individual filaments by varying only the distance to the ionizing source. However, they had to assume that elemental abundances may vary by factors as large as 2 from one filament to another, in order to reproduce the observed spectra. This hypothesis seems unrealistic. Instead, the variation of electronic density should be taken into account, together with variation of distance.

Models 2 and 3 were computed in order to give an idea of the scatter in line intensities that one theoretically might expect from one filament to another.

In Model 2, n_H is 4×10^3 cm^{-3}, and the distance to the source is 2×10^{18} cm; in Model 3, n_H is 5×10^2 cm^{-3} and the distance to the source is 8×10^{18} cm. By comparing the line intensities relatively to Hβ given in lines 5 and 6 of Table 2, we see that [O III] λ 5007/Hβ varies from ~ 2 to ~ 35. Woltjer[5] does not report values of this ratio smaller than ~ 10. This may be due to observational selection, since such low ratios as 2 should be found in filament which are rather distant fromthe source, and therefore presenting a smaller surface brightness. Still, his spectra show [O III] λ 5007/Hβ ratios varying between ~ 10 and ~34. The scatter in the [O II] λ 3727/Hβ ratios obtained in Models 1, 2 and 3 is only between ~ 15 (Model 1) and ~ 9 (Models 2 and 3). Indeed, there is a non negligible part of O in form of O^+ in all three models; besides, models of high excitation have a higher temperature ($T_e \simeq 9300$ °K for Model 2), therefore the [O II] line emissivity is enhanced in models where

the O^+ ion is less abundant. However, [O II] λ 3727 / Hβ ratios up to 30 are observed by Woltjer[5] suggesting that an additional mechanism recombining O^{++} is at work. Charge transfer reactions between O^{++} and H^0 as proposed by Péquignot *et al.*[7] are a good candidate.

5. THE INFLUENCE OF A DILUTED MEDIUM ON THE EMISSION LINE SPECTRUM

All models of filaments constructed sofar predict a value for the He II λ 4686 line intensity which is much weaker than observed. It is probable that part of the excess in the He II line may be explained by blending with the [Fe III] λ 4658 line[4]. However, it is not unreasonable to think that part of the He II λ 4686 line may be emitted not by the filaments, but by a diluted medium in which they are bathing. This has been suggested already by Davidson[3], yet the importance of this phenomenon has not been estimated.

To test this possibility, we built a spherical model with $n_H = 10\ cm^{-3}$, representing the diluted medium around the ionization source (with the same elemental abundances and source characteristics as previously). The temperature and ionization structure are displayed in Figures 4 and 5

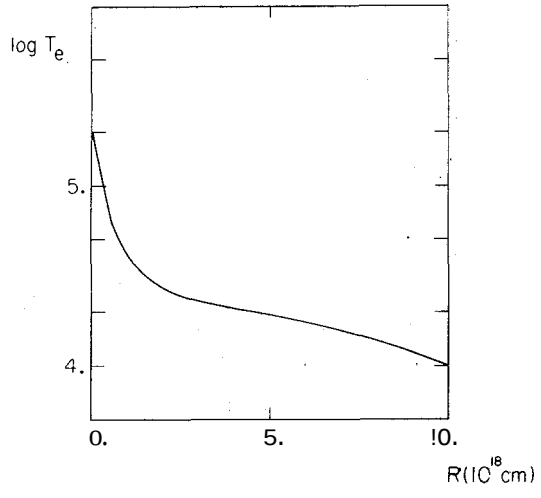

Fig. 4 - Electronic ternperature of the diffuse medium versus distance R to the centre.

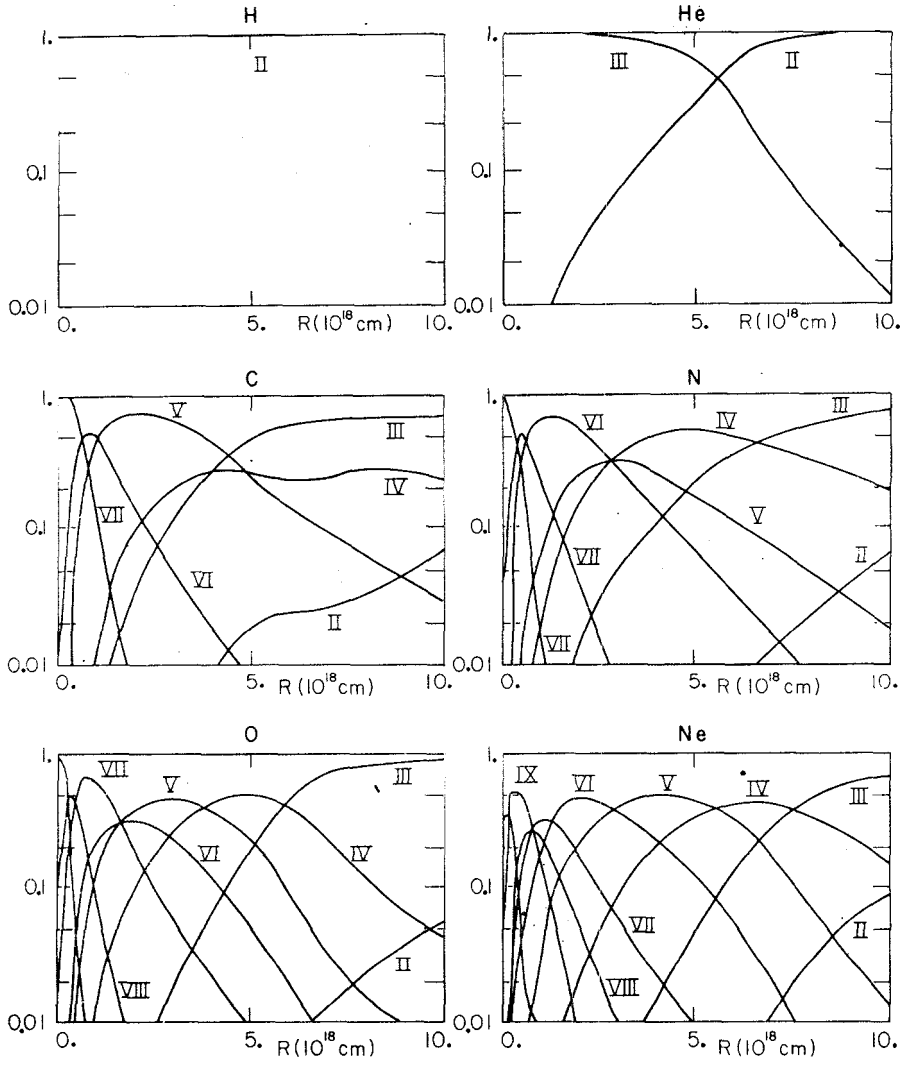

Fig. 5 - Fractional abundance of the ions in the diffuse medium versus R.

respectively. The line intensities relatively to Hβ emitted within a radius 4.9×10^{18} cm (corresponding approximately to the dimensions of the filamentary structure of the Crab Nebula) are reported in line 7 of Table 2.

The luminosity in Hβ corresponding to the same radius is 4.8×10^{33} ergs /s.

The intensity of a line λ relatively to Hβ, integrated over the whole nebula (filaments and diffuse medium) is given by:

$$\frac{I_{\lambda_{f+d}}}{I_{H_{\beta_{f+d}}}} = \frac{I_{\lambda_f}}{I_{H_{\beta_f}}} \frac{I_{H_{\beta_f}}}{I_{H_{\beta_{f+d}}}} + \frac{I_{\lambda_d}}{I_{H_{\beta_d}}} \frac{I_{H_{\beta_d}}}{I_{H_{\beta_{f+d}}}} \qquad (9)$$

where I_A and I_{H_β} are the intensities of the lines A and Hβ respectively, the subscripts f and d referring to filaments and diffuse medium respectively. Then, remembering that the total luminosity in Hβ is 3.39×10^{34} ergs/s [34], we obtain the values reported in line 8 of Table 2, if we assume that all filaments can be represented by Model 1. We see that He II λ 4686 / Hβ is larger than in Model 1 (the average filament) by a factor 5. The only other line ratios which are significantly different (and larger) from those of Model 1 are those concerning C IV λ 1549, C III λ 1909 and to a lesser extent [O III] λ 4363, which is enhanced by the higher temperature in the diluted medium. Unfortunately, none of these lines have been observed. But our result that the other line ratios are not different from those of Model 1 is in agreement with the fact that the line intensities integrated over the whole nebula, which have been measured by Kirshner[34] for [O II], [O III] and [N II] are similar, when divided by $I_{H\beta}$ to the values found by Woltjer[5] and Trimble[6] for the filaments.

When one observes a filament, especially when the slit of the spectrograph is larger than the filament's apparent dimensions the spectrum is contaminated by the light emitted by the diffuse gas which lies nearby the filament and on the line of sight, and the $I_{He\ II}/I_{H\beta}$ line ratio obtained in the spectrum is larger than the ratio of the He II and Hβ lu-

minosities of the filament itself, although the effects is much weaker than in the case of overall observations of the nebula. As a quantitative example, consider a filament which Hβ surface brightness averaged over the slit width is 2×10^{-4} ergs/cm^2/s, a typical result of Woltjer's observation[5] (The real surface brightness of the filament itself is larger). At a projected distance of the centre of 4×10^{18} cm, the Hβ emissivity of the diffuse medium integrated on the line of sight ascomputed in our model is 4.5×10^{-6} ergs/cm^2/s and He II A $4686_d/H\beta_d = 4.2$. From the $He\ II_f/H\beta_f$ ratio of Model 1 (equal to 0.17), and using Equation (9), we find that the observed He II A 4686 / Hβ ratio would be equal to 0.26. At a projected distance to the centre of 1×10^{18} cm, we obtain He II h 4686 / Hβ ≃ 4.7 for the diffuse medium, and an integrated Hβ emissivity of 7.3×10^{-6} ergs/cm^2/s; the observed He II A 4686 / Hβ ratio would then be equal to 0.33.

These results show that it is quite possible that the He II λ 4686 line intensities reported by Woltjer[5] do not refer to the filaments themselves, but include a non negligible contribution of a diluted gas, in addition to the blending with the [Fe III] λ 4658 line.

6. FINAL REMARKS

We do not pretend having built a proper model of the Crab Nebula. We only emphasized that a detailed model should try to account for individual filaments, by varying their distance to the ionizing source and their gas density. Besides, we showed that the discrepancy between the high He II h 4686 / Hβ line ratio claimed to be observed in the filaments, and the much lower value found in all models of filaments which were computed sofar can be partly explained by a contribution to the He II line of a diluted medium in which the filaments are bathing, apart from a contamination by a [Fe III] line at h 4658 Å. In order to verify this point, more detailed observations with high angular resolution are needed, especially concerning the He II h 4686 and [O III] A 4363 lines. The ultra-violet line intensities of C IV h 1549 and CIII] λ 1909 would also be helpful.

On the theoretical side, a more complete study should determine the density of the diluted medium and investigate the consequences on the spectra emitted by the filaments of a softening of the incident radiation due to the fact that the diluted gas converts photons with energies greater than about 100 eV into photons of energies 54.4 eV, and the photoionization of 2s subshells, which has been neglected here, might affect the ionization equilibrium. Besides, charge transfer reactions, as proposed by Péquignot *et* a ~ . if, they are confirrned, should be taken into account in future models, since they may be the dominantprocessfor recombining certain ions.

Note

In an article concerning the optical emission of Cygnus A (Osterbrock, D.E. and Miller, J.S. Ap. J. 197, 535 (1975) the authors give some information on scanner measurements performed by Miller on the Crab Nebula. In the last line of Table 2, we reproduce their figures which are averages between the lines intensities corrected for interstellar extinction of a "red" filament and those of a "green" filament. Their values are quite similar to those which we adopted for the "mean" filament. They measured the [O III] A 4363 line intensity and their observed [O III] A 4363 / [O III] λ 5007 ratio is somewhat larger than the one found in our models, indicating a higher temperatures, which will have to be accounted for in future studies.

REFERENCES

1. Williams, R.E., Astrophys, J. 147, 556 (1967).
2. Davidson, K., Tucker, W., Astrophys. J. 161, 437 (1970).
3. Davidson, K., Astrophys. J. 186, 223 (1973).
4. Contini, M., Kozlovsky, B.Z., Shaviv, G., Astron.Astrophys. 59, 387 (1977).
5. Woltjer, i., B.A.N. 14, 39 (1958).
6. Trimble, V., Astronomical J. *75*, 926 (1970).
7. Pequignot, D., Aldrovandi, S.M.V., Stasinska, G. Astron. Astrophys., in press. (1977).

8. Stasinska, G., Astron. Astrophys. in press (1977).
9. Stasinska, G., Astron. Astrophys. in press (1977).
10. Tarter, C.B., Ph. D. Thesis, Cornell University (1967).
11. Mac Alpine, G.M., Ph. D. Thesis, University of Wisconsin (1972).
12. Tarter, C.B., Salpeter, E.E., Astrophys. J. 156, 953 (1969).
13. Osterbrock, D.E., Astrophysics of Gaseous Nebulae (San Francisco ; Freeman) (1974).
14. Aldrovandi, S.M.V., Pequignot, D., Astron.Astrophys. 25, 137 (1973).
15. Bergeron, J., Collin-Souffrin, S., Astron. Astrophys. 36, 27 (1974).
16. Seaton, M.J., Rep. Prog. Phys. 23, 313 (1960).
17. Seaton, M.J., M.N.R.A.S. 119, 81 (1959).
18. Hummer, D.G., Seaton, M.J., M.N.R.A.S. 127, 217 (1964).
19. Mac Guire, E.J., Phys. Rev. 185, 1 (1969).
20. Tucker, W.E., Gould, R.J., Astrophys. J. 144, 244 (1966).
21. House, L.L., Astrophys. J. Suppl. 8, 307 (1964).
22. Bergeron, J., Collin-Souffrin, S., Astron.Astrophys. 25, 1 (1973).
23. Aldrovandi, S.M.V., Pequignot, D., Astron. Astrophys. 47,321 (1976).
24. Aldrovandi, S.M.V., Pequignot, D., Astron. Astrophys. 23, 33 (1976).
25. Johnson, L.C., Astrophys. J. 174, 227 (1972).
26. Wiese, W.L., Smith, M.W., Glennon, B.M., *Atomic Transition Probabilities*, Vol. 2, NSRDS-NBS4 (1966).
27. Wiese, W.L., Smith, M.W., Miles, B.M., *Atomic Transition Probabilities*, Vol. 2, NSRDS-NBS4 (1969).
28. Nussbaumer, H., Astrophys. J. 166, 411 (1971).
29. Garstang, R.H., Shamey, L.J., Astrophys. J. 148, 665 (1976).
30. Brocklehurst, M., M.N.R.A.S. *153*, 471 (1971).
31. Brocklehurst, M., M.N.R.A.S. 157, 211 (1972).
32. Krogh, F.T., Variable order integrators for the numerical solution of ordinary differential equations, JPL Document N? CP-2308, NPO-11643, California Institute of Technology (1970).
33. Trimble, V., Astron. J. 73, 535 (1968).
34. Kirshner, R.P., Astrophys. J. 194, 323 (1974).
35. Miller, J.S., Astrophys. J. 180, L83 (1973).
36. Minkowsky, R., Astrophys. J. 96, 199 (1942).
37. Osterbrock, D.E., P.A.S.P. 69, 227 (1957).
38. Field, G.B., Steigman, G., Astrophys. J. 166, 59 (1971).